VOL. 16, NO. 18, SEPTEMBER 2021 ISSN 1819-6608
ARPN Journal of Engineering and Applied Sciences

www.arpnjournals.com

ASSESSMENT OF CURRENT GENERATED IN A PHOTO-ELECTROCHEMICAL CELL USING N-TIO_2/CU_2O ELECTRODES AND STAINLESS STEEL AS WORKING ELECTRODE

Álvaro Realpe, Breanda Chamorro and María T. Acevedo
Department of Chemical Engineering, Research Group of Modeling of Particles and Processes,
University of Cartagena, Campus Piedra Bolívar, Cartagena, Colombia
E-Mail: arealpe@unicartagena.edu.co

ABSTRACT

N-doped TiO_2 and Cu_2O nanoparticles were synthesized through a chemical reduction of the titanium (IV) isopropoxide and copper (II) sulfate 5-hydrate, respectively. TiO_2 nanoparticles were doped with N at different concentrations (10, 20 and 30% wt.) to modify its optical properties. The photoactivity of the elaborated photoelectrode was analyzed by means of photocurrent generation and UV-Vis spectroscopy. The bandgap energy of the N-doped TiO_2photoelectrode decreased with increasing N concentration and the Cu_2O photoelectrode has the energy value of the lowest bandgap, 2.1 eV. Furthermore, Cu_2O photoelectrode generates higher photocurrent than N-doped TiO_2 electrodes.

Keywords: band gap, copper oxide, N-doping, titanium dioxide, photoelectrode.

INTRODUCTION

Energy is considered as a fundamental source for innumerable productive processes that have allowed throughout history the industrialization as well as improve the living standards of society. Due to the increasing energy demand a lot of alternative processes for energy generation through clean mechanism and use of renewable sources are been developed by different researcher [1]-[4]. Photo-electrochemical water splitting is a promising alternative for using of solar energy and the sustainable hydrogen production as an energy carrier [5], which involves different physicochemical process. First a light absorption process occurs by the semiconducting photoelectrode, a pair of charge carriers, electrons-holes are generated and the electrons are excited to conduction band, after that, the separation and transportation process takes place and finally the last process is the surface reactions where redox reactions occur and the hydrogen is produced [6]. In these devices the semiconductor photoelectrode is the main component since as has a decisive influence on the solar energy to hydrogen conversion. Among semiconductor, metal oxides are very attractive materials due to their chemical stability, suitable band gap positions and low cost [7]. Different metal oxides have a wide distribution of the band gap energy, band edge positions and presents electronic characteristics of n-type or p-type semiconductor. In the present investigation the effect of the N doped concentration on optical properties of TiO_2 nanoparticles has been studied and compared with the optical behavior of the p type of semiconductor Cu_2O synthesized through a chemical reduction mechanism. Through impregnation wet method were doped TiO_2 nanoparticles with N atoms and by using the doctor blade technique were prepared TiO_2, N-TiO_2 and Cu_2O films.

MATERIALS AND METHODS

Poly For synthesis stages were used different chemicals substances, such as Titanium (IV) isopropoxide (Merk), Ammonium chloride (NH4Cl, SIGMA-ALDRICH), copper (II) sulfate 5-hydrate (PanReac) sodium hydroxide, D(+) - Glucose anhydrous (Merk) and sodium sulfate anhydrous (Alfa Aesar).

Synthesis of TiO_2 Nanoparticles

TiO_2 nanoparticles were prepared by chemical reduction method using a natural extract of lemon grass [8], [9]. Leafs of lemon grass were cutted in small pieces and washed with abundant water, after that, the organic material was dried in an oven at 50°C, and it was ground. To prepare the lemon grass extract, 100 g of grounded biomass was submerged in 500 ml of distilled water at 90 °C. After 3 hours, it was filtered to remove the organic material and the aqueous solution was concentrated by evaporation in a plate for heating at 60 °C and 500 rpm.

Titanium (IV) isopropoxide $[Ti[OCH(CH_3)_2]_4]$ solution (20mM) was prepared by dissolving it in distilled water by using ultrasonic agitation during 30 minutes. The lemon grass extract was slowly dripped into $[Ti[OCH(CH_3)_2]_4]$ solution and the mixture was stirred continuously for 24 h at room temperature. The precipitate resulting from the reaction was allowed to settle down and then it was centrifuged and washed with ethanol and water individually. Finally, the nanoparticles were calcined in a muffle at 550°C for 3 h.

Preparation of N-doped TiO_2 Nanoparticles

N-doped TiO_2 was prepared by wet impregnation method; NH_4Cl was used as the N source. TiO_2 nanoparticles were suspended on deionized water and sonicated during 30 min to dissolve the semiconductor. This was followed by the addition of aqueous solutions (deionized water) with the required amount of precursor NH_4Cl and a sonication step for 1 hour, during this time

the color of the mixture changed into yellowish. Various amounts of nitrogen doping were prepared at 10, 20 and 30 %. Then, the doped samples were stirred for 2 hours at 80 °C. After, the solvent was evaporated, and finally, the samples were calcined in a muffle furnace at 400°C for 2 hours [10].

Preparation of Cu_2O Nanoparticles

Cu_2O nanoparticles were synthesized by a chemical reduction route [11]. Aqueous solutions (distilled water) of copper sulfate (0.14 M), sodium hydroxide (0.75 M) and glucose (0.5 M) were prepared. 100 ml of NaOH solution were added to 100 ml of the precursor solution and it was stirred at ambient temperature, after that, 40 ml of glucose solution were added and mixing under the same temperature condition during 2 h. During this process, the color of solution gradually changed into brick-red color. The resultant solution was kept on rest for 2 hours, then the precipitate nanoparticles were centrifuged at 4000 rpm for 15 min for removing the supernatant and washed with ethanol and distilled water in turn.

Elaboration of Photoelectrodes

Thin films of semiconductor materials were supported over stainless steel sheets, the suspension was prepared by adding nanoparticles to acronal solution (50% v/v distilled water - acronal), the suspension was magnetically stirred for 30 min, and an ultrasonic bath was used to improve the dispersion of nanoparticles. The paste was applied onto the stainless steel sheet by doctor blade technique and the thin film was allowed to dry in air for some minutes, this process was repeated two more times to obtain a multilayer film (three layers), after that, films were subject to thermal treatment of sintering at 400°C for 30 min to improve the nanoparticles connectivity, mechanical strength and the electrical conductivity of the photoelectrodes [12].

UV-VIS/RDS Characterization of Synthesized Nanoparticles

UV-Visible Reflectance Spectra were carried out in a spectrophotometer UV/VIS Evolution 600 Thermo Scientific. The measurements were recorded in the wavelength range from 200 to 800 nm. The band gap of TiO_2, N-TiO_2 and Cu_2O nanoparticles was determined by using the Tauc equation indicated below.

$$\alpha h\upsilon = B(h\upsilon - Eg)^n \quad (1)$$

where α is the absorption coefficient, Eg the band gap energy, υ is the light frequency (s^{-1}), B is the absorption constant, n is a constant and h is the Planck's constant (J.s). n is related to the electronic interband transition. The band gap energy value is obtained by plotting $(\alpha h\upsilon)1/n$ as a function of E (photon energy) and extrapolating until $(\alpha h\upsilon)^{1/n} = 0$ the linear section of this spectra [12].

Electrochemical Measurements

Photocurrent characteristics of the elaborated photoelectrodes were measured in a configuration of two electrodes into a photo-electrochemical cell with a N-TiO_2 or Cu_2O electrode and a stainless steel as working electrode, as shown in the Figure-1. The photoelectrodes were introduced in an aqueous 0.5 M Na_2SO_4 electrolyte solution and radiated with a source of visible light by using a cell system. The measurement of the electrical parameter was carried out using a multimeter connected to the system through an external circuit, electrical contact was made with a copper wire [12].

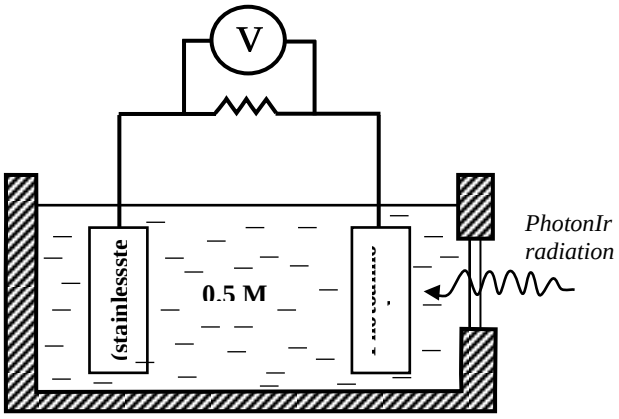

Figure-1. System of photoelectrochemical cell for water splitting used in the study.

RESULTS AND DISCUSSIONS

Figure-2 shows the pure TiO_2 and N-TiO_2 nanoparticles synthesized by a green chemical reduction method and doped with different concentrations of nitrogen. The yellowish color in each sample is intensified with the increase of the nitrogen atom concentration. The Figure 3 shows the Cu_2O pure nanoparticles synthesized.

Figure-2. Synthesized TiO_2 nanoparticles: a.) Pure TiO_2, b.) N-TiO_2 10% wt, c.) N-TiO_2 20% wt, d.) N-TiO_2 30% wt.

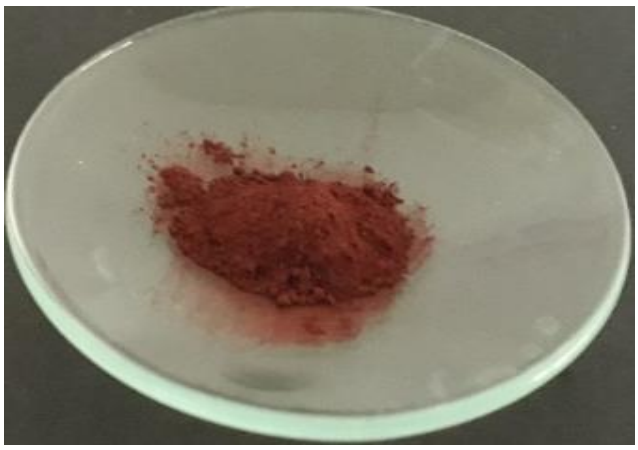

Figure-3. Synthesized Cu_2Onanoparticles

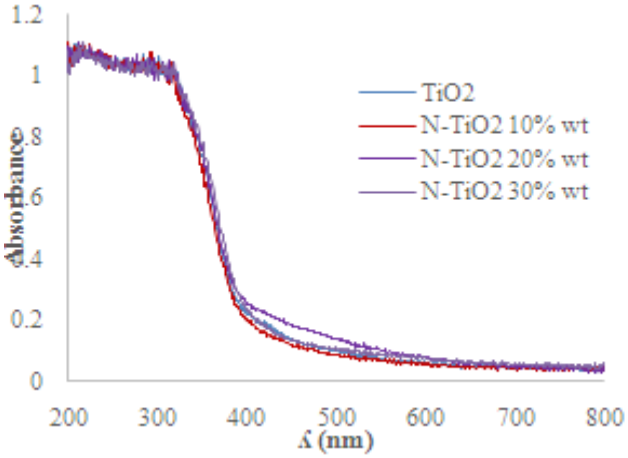

Figure-4. UV-VIS/RDS spectrum of TiO_2 and N-doped TiO_2 nanoparticles.

UV-VIS Diffuse Reflectance Spectroscopy of TiO_2 and N-TiO_2 Nanoparticles

Figure-4 shows UV-Vis diffuse reflectance spectra of N-doped TiO_2 and undoped TiO_2. The intensity of the absorbance was similar for N-TiO_2 nanoparticles compared to the pure TiO_2. The highest absorbance was recorded between 200 and 400 nm, it is a typical behavior for TiO_2 samples, and however, an absorption band is present in the visible region around 400 - 600nm.

For an indirect allowed optical transition band to band in TiO_2 [12], it was plotted $(\alpha h\upsilon)1/2$ as a function of hv (photon energy), the band gap energy calculated for pure and 10% wt, 20% wt and 30% wt N-doped TiO_2 samples is 2.8 eV, 2.75 eV, 2.72 eV, 2.69 eV respectively.

Figure-5 shows that the band gap energy decreases with doping and with the increasing of the N concentration, the N-doped sample with higher concentration showed a decrease in the optical absorption edge by around 0.11 eV. The band gap energy for the different doping samples decreases linearly with N concentration, showing a small change for each one, as it was reported by [13] for different N doped concentrations. The band gap reduction for N doping occurs due to the N atoms weave into the TiO_2 lattice and induce new band states between the valence and conduction bands, through replacing the sites of O atoms [14].

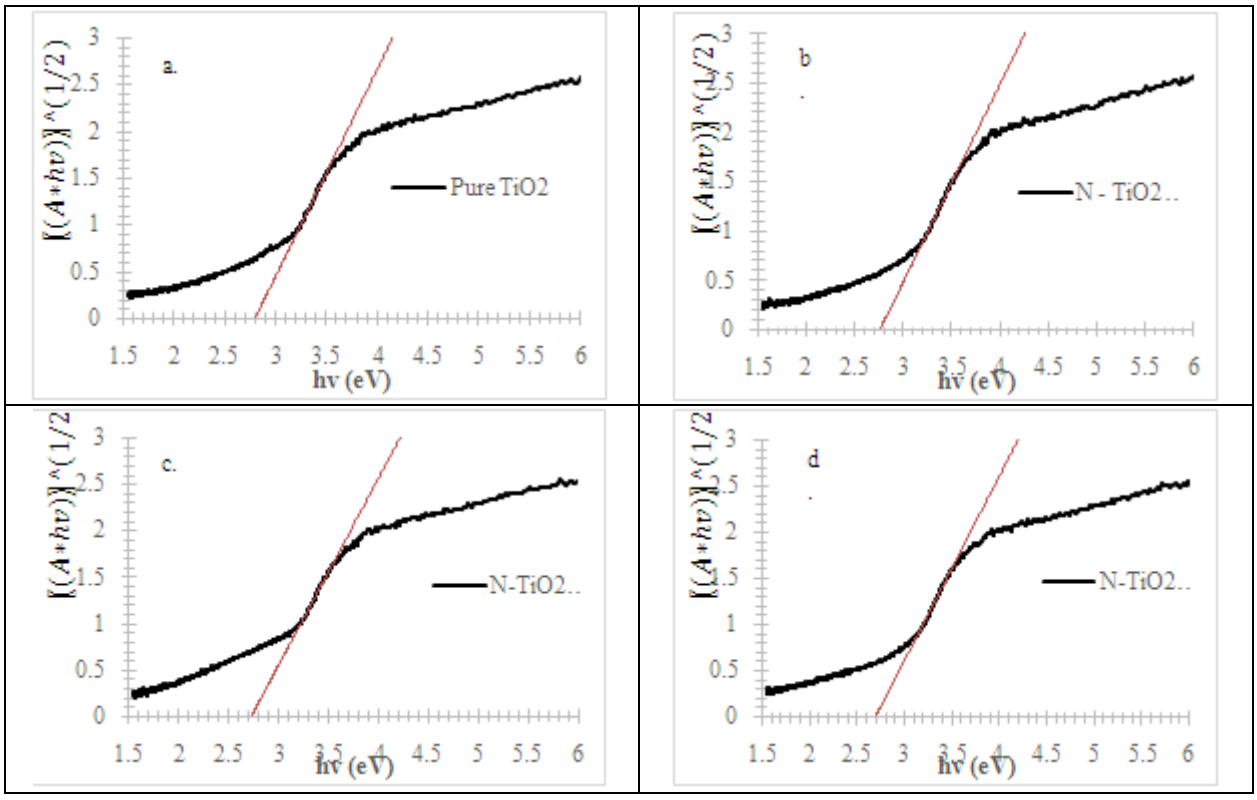

Figure-5. Tauc's plot undoped TiO_2 and doped TiO_2 a) Pure TiO_2, b) N-TiO_2 10 % wt., c) N-TiO_2 20 % wt. d) N-TiO_2 30 % wt.

UV-VIS Diffuse Reflectance Spectroscopy of Photoelectrodes Cu_2O

Figure-6 shows the absorption spectra in the range 200-800 for the cuprous oxide nanoparticles synthesized. The spectra show a characteristic absorption peak around 560 nm, as a result of the band transition in Cu_2O nanoparticles, which is good agreement with the absorption edge values reported previously [17]. According to Sathiya *et al*. [18] the broad band in the region between 420 and 580 nm reveals the Cu_2O nanoparticles formation and the position of this band relies on size, shape and dielectric environmental of the nanoparticles. It is also shows that the absorbance decreases with increasing wavelength, however, high absorbance values were observed in the visible region.

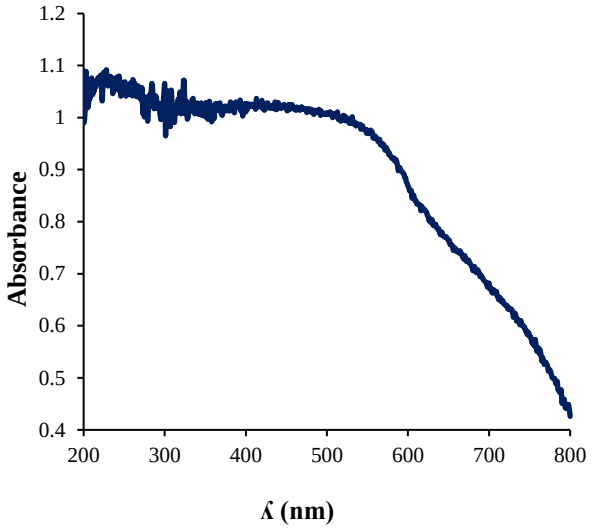

Figure-6. UV-VIS/RDS spectrum of Cu_2O nanoparticles synthesized.

As was previously expressed the band gap energy of synthesized nanoparticles was calculated by using the Tauc's Plot method from the relationship between absorption coefficient and photon energy. The cuprous oxide system is a p type semiconductor characterized by a direct electronic transition from valence band to conduction band [17], so when plotting $(\alpha h\upsilon)^2$ as a function of hv (photon energy) it is obtained the absorption edge of Cu_2O nanoparticles, as shown in Figure-7. The Eg value obtained from the plot is 2.1 eV, which reveals that the synthesized material can be activated by visible light, this value is similar to the obtained value for energy band gap with different synthesis process [16], [19-20].

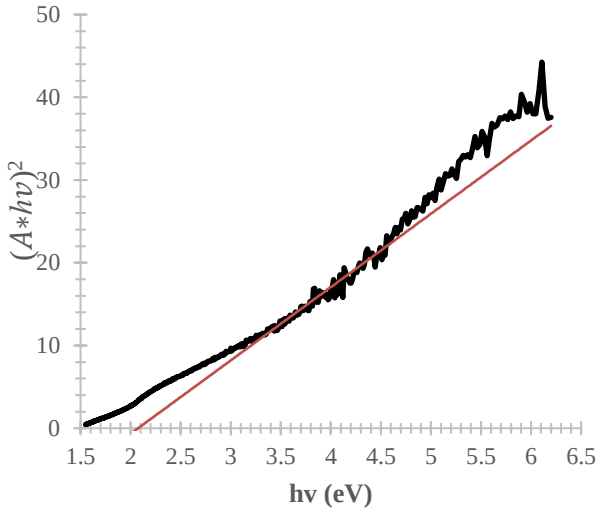

Figure-7. Tauc's plot of pure Cu_2O.

Photocurrent Measurements

In Figure-8, the photocurrent response is registered for the pure TiO_2 and different non-metal doped TiO_2 samples during the UV-V irradiation. All doped TiO_2 samples with non-metal exhibit higher photocurrents than pure TiO_2 (Figure-8b); however, the sample with 30% N-doped showed a decrease in generated photocurrent.

The improvement of its electrical properties is due to the incorporation of nonmetal that allows minimizing the recombination of the photogenerated charge carriers e-/h+, moreover, the decrease in the generation of photocurrent at the highest N concentration could be associated with the location of the dopant. According to Amrani *et al*. [13] the low photocurrent of N-doped TiO_2photoelectrodes is frequently attributed to the electron-hole recombination caused by the N-induced state below the conduction band, due to diffusing charge carriers can recombine at dopant sites and the input energy is lost.

In Figure-8a is observed also the photocurrent response of Cu_2O nanoparticles synthesized under the same operation conditions, where the photocurrent values for these photoelectrodes were higher than all the TiO_2 samples, which can be attributed to the high absorption capacity in the visible region due to its low bang gap energy and the band energy position, its conduction band is above the water reduction potential, making it suitable for water splitting without external bias in the cell [21], furthermore, TiO_2 has a hole diffusion length of around 10 nm which would increase the recombination possibility [22].

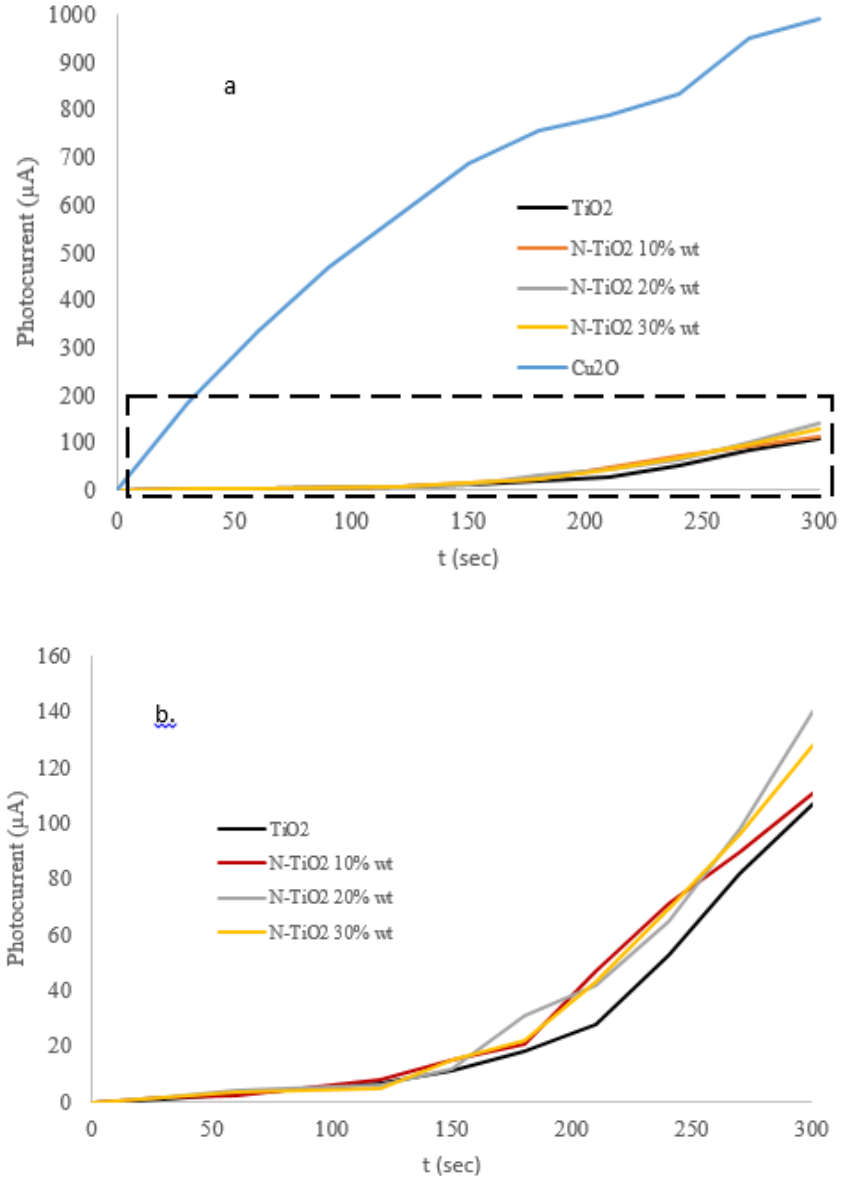

Figure-8. Photocurrent as a function of time without bias voltages under illumination by visible light. a) TiO_2, N-Doped TiO_2 and CuO_2 electrodes, b) enlargement of the bordered section for TiO_2 and N-doped TiO_2 electrodes.

CONCLUSIONS

N-doped TiO_2 nanoparticles were successfully prepared by green synthesis method using a natural extract of lemon grass. The band gap energy of the N-doped TiO_2 nanoparticles decreases with increasing nitrogen concentration. The lowest value of band gap energy was 2.69 eV at 30% N-doped TiO_2, meanwhile the band gap energy for Cu_2O nanoparticles was 2.1 eV. According to these results, all synthesized nanoparticles have a good behavior under visible light irradiation. The higher value for photocurrent generation was obtained for Cu_2O photoelectrode, 992 µA, this result prove that this semiconductor has suitable properties to be used as working photoelectrode for photoelectrochemical water splitting.

ACKNOWLEDGEMENTS

Authors of this paper would like to express their gratitude to University of Cartagena for providing the resources and the space to perform this project through the grant number No. 089-2019.

REFERENCES

[1] Hori K., Matsui T., Hasuike T., Fukui K., Machimura T. 2016. Development and application of the renewable energy regional optimization utility tool for environmental sustainability: REROUTE, Renewable Energy. 93, 548-561.

[2] Realpe A., Garzon J., Montes D. 2017. Mathematical Modelling of Electric Energy Potential of Piedra Bolivar Campus of Cartagena University, Obtained from Solar Radiation. International Journal of Chem Tech Research. 10(1): 209-214.

[3] Baldiris I., Acosta J., Mendoza D., Fajardo J., Realpe A. 2018. Tibaquirá, J., Pem Fuel Cell Performance Assessment using exergoeconomics, Analysis, Contemporary Engineering Sciences. 11(5): 203-214.

[4] Realpe A., Diazgranados J., Acevedo M. 2012. Electricity Generation and Wind Potential Assessment in Regions of Colombia, DYNA. 79(171): 116-122.

[5] Landman A., Dotan H, Shter G., Wullenkord M., Houaijia A., Maljusch A., Grader G., Rothschild A. 2017. Photoelectrochemical water splitting in separate oxygen and hydrogen cells. Nature Materials. 16, 646-651.

[6] C. Jiang, S. Moniz, A. Wang, T. Zhang, J. Tang, Photoelectrochemical devices for solar water splitting - materials and challenges, Chem. Soc. Rev. 46(15): 4645-4660, June 2017.

[7] R. Marschall, L. Wang, Non-metal doping of transition metal oxides for visible-light photocatalysis, Catalysis Today. 225: 111-135, April 2014.

[8] Realpe A., Nuñez, D., Rojas, N., Ramirez, Y., Acevedo, M., 2021, Effect of Fe-N Codoping on the Optical Properties of TiO_2 for Use in Photoelectrolysis of Water. ACS Omega. 6(7): 4932-4938.

[9] Realpe A., Núñez D., Acevedo M. 2017. Effect of Cu on Optical Properties of TiO_2 Nanoparticles. Contemporary Engineering Sciences. 10(31): 31, 1539-1549.

[10] Yoong L., Chong F., Dutta B. 2009. Development of copper-doped TiO_2photocatalyst for hydrogen production under visible light, Energy. 34(10): 1652-1661.

[11] Amrani M., Srikanth V., Labhsetwar N., Fatesh A., Shaikh H. 2016. Phoenix dactylifera mediated green synthesis of Cu_2O particles for arsenite uptake from water. Sci Technol Adv Mater. 17(1): 760-768.

[12] López L., Gómez R. 2012. Band-gap energy estimation from diffuse reflectance measurements on sol-gel and commercial TiO_2: a comparative study. Journal of Sol-Gel Science and Technology. 61(1): 1-7.

[13] Yalçin, Y., Kılıç, M., Cinar, Z., 2016, The Role of Non-Metal Doping in TiO_2Photocatalysis. Journal of Advanced Oxidation Technologies. 13(3): 281-296.

[14] Matsuda, A., Krengvirat, W., 2013, Well-aligned TiO_2 nanotube arrays for energy-related applications under solar irradiation. Journal of Asian Ceramic Societies. 1(3): 203-219.

[15] Suzuki K., Tanaka N., Ando A., Takagi H. 2011. Optical Properties and Fabrication of Cuprous Oxide Nanoparticles by Microemulsion Method. Journal of the American Ceramic Society. 94(8): 2379-2385.

[16] Behera M., Giri G. 2104. Green synthesis and characterization of cuprous oxide nanoparticles in presence of a bio-surfactant. Materials Science-Poland. 32(4): 702-708.

[17] Sathiya S., Okram G., Jothi Rajan M. 2017. Structural, Optical and Electrical Properties of Copper Oxide Nanoparticles Prepared through Microwave Assistance. Advanced Materials Proceedings. 2(6): 371-377.

[18] Rafea M., Roushdy N. 2008. Determination of the optical band gap for amorphous and nanocrystalline copper oxide thin films prepared by SILAR technique. Journal of Physics D: Applied Physics. 42(1).

[19] Gondal M., Qahtan F., Dastageer M., Maganda W., Anjum D. 2013. Synthesis of Cu/Cu_2O Nanoparticles by Laser Ablation in Deionized Water and Their Annealing Transformation IntoCuO Nanoparticles. Journal of Nanoscience and Nanotechnology. 13(8): 5759-5766.

[20] Azadi H., Aghdam H., Malekfar R., Bellah S. 2019. Effects of energy and hydrogen peroxide concentration on structural and optical properties of CuOnanosheets prepared by pulsed laser ablation. Results in Physics. 15.

[21] Qi H., Wolfe J., Fichou D., Chen Z. 2016. Cu_2O Photocathode for Low Bias Photoelectrochemical Water Splitting Enabled by NiFe-Layered Double Hydroxide Co-Catalyst. Scientific Reports. 6(3).

[22] Ynag Y., Han D., Liu T., Wang G., Li Y. 2017. Progress in Developing Metal Oxide Nanomaterials

for Photoelectrochemical Water Splitting. Advanced Energy Materials. 7(19): 1-26.